



1,2,4-Triazole derivatives as host materials for blue and green phosphorescent organic light-emitting devices

Huixia Xu^{a,b,*}, Peng Sun^{a,b}, Kexiang Wang^{a,b}, Yanqin Miao^{a,b}, Tingting Yang^{a,b}, Hua Wang^{a,b}, Bingshe Xu^{a,b}, Wai-Yeung Wong^{a,c}

^a Key Laboratory of Interface Science and Engineering in Advanced Materials, Ministry of Education, Taiyuan University of Technology, Taiyuan 030024, PR China

^b Shanxi Research Center of Advanced Materials Science and Technology, Taiyuan 030024, PR China

^c Institute of Molecular Functional Materials, Department of Chemistry and Institute of Advanced Materials, Hong Kong Baptist University, Waterloo Road, Hong Kong, China

ARTICLE INFO

Article history:

Received 5 April 2016

Received in revised form 1 June 2016

Accepted 3 June 2016

Available online xxx

Keywords:

Host materials

Light-emitting device

Carbazole

ABSTRACT

A novel host material, namely 9-(6-(3-phenyl-5-(pyridin-2-yl)-4H-1,2,4-triazol-4-yl)hexyl)-9H-carbazole (PPHCZ) was designed and synthesized by incorporating 1, 2, 4-triazol as the electron-withdrawing moiety and carbazole as electron-donating moiety using hexyl as bridge. The photophysical, electrochemical, thermal properties and performances in phosphorescent organic light-emitting devices (PhOLED) were thoroughly characterized. PPHCZ with a high triplet energy level (3.01 eV) exhibited an obvious intermolecular interaction in thin film. Green and blue PhOLEDs using *fac*-tris(2-phenylpyridine) iridium and iridium(III) bis(4,6-difluorophenyl)-pyridinato $-N,C^{2'}$]picolinate as phosphorescent dopants have been fabricated.

© 2016 Published by Elsevier Ltd.

1. Introduction

Phosphorescent organic light-emitting devices (PhOLED) have attracted considerable interests due to their high efficiency and great applications in the next generation full-color flat-panel displays.^{1–3} In the design of highly efficient PhOLEDs, the selection of a proper host material is of great importance. In general, to prevent back energy transfer from dopant to host, the host materials should have a wider energy gap (E_g) and larger triplet level (E_T) than dopant.⁴ Therefore, to attain efficient blue PhOLEDs, the development of appropriate host materials has become a challenge because of intrinsic wide E_g of blue-emitting dopant.^{5,6}

Bipolar hosts with electron-donating and electron-withdrawing moieties have drawn much attention due to excellent charge-transport capabilities to make the charge recombination zone within the emissive layer.^{7,8} Carbazole possessing high triplet energy level ($E_T > 2.9$ eV) and excellent electron-donating properties were widely used as the structural moieties in blue hosts. Several bipolar hosts for sky-blue phosphorescent devices were reported including oxide/carbazole,⁹ pyrimidine/carbazole¹⁰ dibenzothio-

phene and dibenzofuran/carbazole hybrids et al.^{11,12} The 1,2,4-triazole derivatives have been proved to be excellent electron-transport and hole-block materials due to the electron-deficient triazole moiety.^{13,14} J. Zhuang et al. in 2013 reported an electron-transport material of 3,5-bis(4-(diphenylphosphoryl)phenyl)-4-phenyl-4H-1,2,4-triazole (TPO) with high E_T of 2.86 eV and high glass transition temperature (133 °C).¹⁵

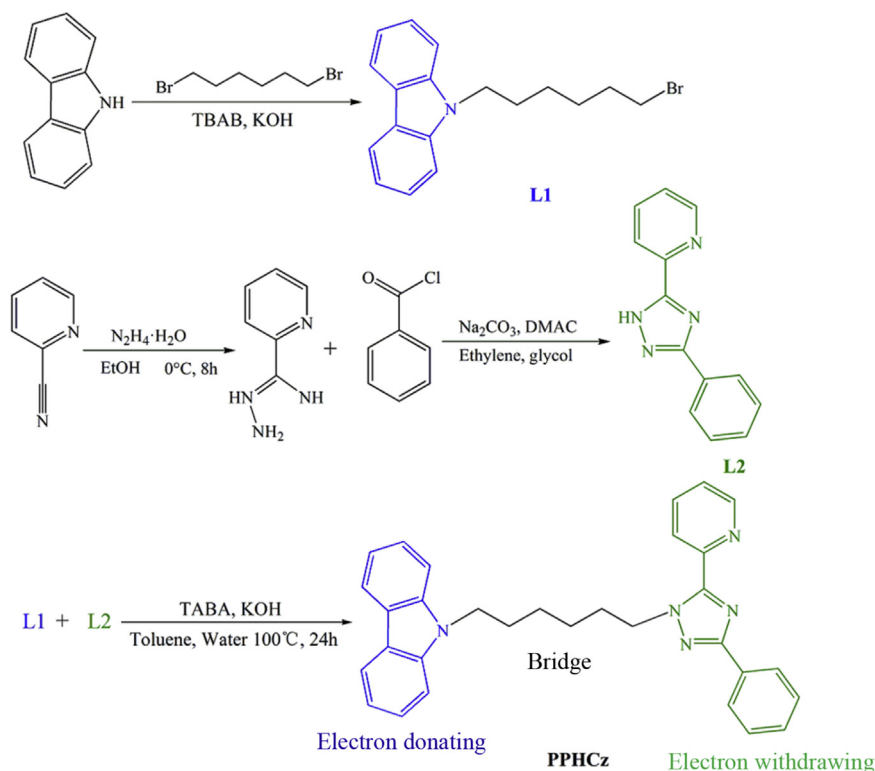
In this paper, we designed and synthesized a novel host material of 9-(6-(3-phenyl-5-(pyridin-2-yl)-4H-1,2,4-triazol-4-yl)hexyl)-9H-carbazole (PPHCz) with the electron-donating carbazole and electron-withdrawing triazole ligands. Two functional groups were connected by hexyl in order to improve the solubility of blue bipolar host. PPHCz can be used as the host matrix to fabricate the green- and blue-emitting PhOLEDs.

2. Experimental

2.1. Syntheses of 9-(6-(3-phenyl-5-(pyridin-2-yl)-4H-1,2,4-triazol-4-yl)hexyl)-9H-carbazole (PPHCZ)

All materials were used as received from commercial suppliers without further purification. Synthetic routes are outlined in Scheme 1.

* Corresponding author. E-mail address: xuhuixia@tyut.edu.cn (H. Xu).



Scheme 1. Molecular structure and synthetic routes of PPHCz.

2.1.1. 9-(6-Bromohexyl)-9H-carbazole (L1). A mixture solution of carbazole (5.0 g, 30 mmol), 1, 6-dibromohexane (36.0 g, 150 mmol), tetrabutyl ammonium bromide (TBAB) (1.0 g, 3 mmol), toluene (40 mL) and KOH (25 mL, 50%) was heated to reflux for 12 h. After cooling to room temperature, the mixture was poured into the water (50 mL) and extracted with CH_2Cl_2 . The organic extracts were washed with water and dried over MgSO_4 . The crude product was subjected to silica gel column chromatography using an 8:1 mixture of petroleum ether and CH_2Cl_2 as the eluent. The white crystals of 9-(6-bromohexyl)-9H-carbazole (7.7 g) were obtained. Yield: 78%, ^1H NMR (600 MHz, CDCl_3): δ 8.11(dt, 2H, $J=7.8$ Hz, 1.2 Hz), 7.47–7.44 (m,

2H), 7.40 (d, 2H, $J=8.4$ Hz), 7.24–7.21 (m, 2H), 4.31 (t, 2H, $J=7.2$ Hz), 3.35 (t, 2H, $J=7.2$ Hz), 1.92–1.78 (m, 2H), 1.50–1.37 (m, 2H).

The synthetic route of 2-(5-phenyl-4H-1,2,4-triazol-3-yl)pyridine (L2) can be found in Ref. 16.

2.1.2. 9-(6-(3-Phenyl-5-(pyridin-2-yl)-4H-1,2,4-triazol-4-yl)hexyl)-9H-carbazole (PPHCz). A mixture of L2 (2.22 g, 10 mmol), TBAB(0.32 g, 1 mmol), and 30 mL toluene were stirred for 30 min. 2 M KOH solution was added and stirred for another 30 min at room temperature under nitrogen atmosphere. The L1, which was dissolved in 10 mL toluene, were added slowly into solution and refluxed for 24 h. The water was added after cooling to room temperature. After removal of the solvent, the residue was purified by column chromatography on silica gel using as the eluent to give a white powder. Yield: 80%. ^1H NMR (600 MHz, CDCl_3) δ 8.52 (ddd, $J_1=4.8, J_2=1.8, J_3=0.9$ Hz, 1H), 8.30 (dt, $J_1=7.9, J_2=1.1$ Hz, 1H), 8.18–8.15 (m, 2H), 8.10 (ddd, $J=7.8, J_2=1.2, J_3=0.7$ Hz, 2H), 7.82 (td, $J=7.8, J_2=1.8$ Hz, 1H), 7.47–7.42 (m, 4H), 7.42–7.39 (m, 1H), 7.37 (dt, $J=8.2, J_2=0.9$ Hz, 2H), 7.29 (ddd, $J=7.6, J_2=4.8, J_3=1.2$ Hz, 1H), 7.22 (ddd, $J=7.9, J_2=7.0, J_3=1.0$ Hz, 2H), 4.87–4.81 (m, 2H), 4.28 (t, $J=7.2$ Hz, 2H), 2.00–1.83 (m, 4H), 1.43 (dd, $J=6.6, J_2=3.0$ Hz, 4H). ^{13}C NMR (600 MHz, CDCl_3): δ 163.59, 151.11, 151.70, 151.13, 143.32, 139.78, 134.15, 131.91, 131.41, 129.25, 128.48, 126.89, 126.80, 125.75, 123.22, 121.66, 111.50, 53.56, 45.78, 32.88, 31.77, 29.72, 29.17. FTIR (KBr, cm^{-1}): 3416, 3049, 2926, 2825, 1590, 1466, 1322, 1227, 1153, 1128, 1015, 920, 846, 793, 723. Anal. Calcd for $\text{C}_{31}\text{H}_{29}\text{N}_5$ (%): C, 78.95; H, 6.20; N, 14.85; found: C, 79.60; H, 6.10; N, 14.62.

2.2. General information

^1H NMR data were recorded with Switzerland Bruker DR \times 600 NMR spectrometers. FTIR spectra were measured with a Nicolet 7199B spectrometer in KBr pellets in the range of 4000–400 cm^{-1} . C, H and N microanalysis were carried out with an Elemental Vario

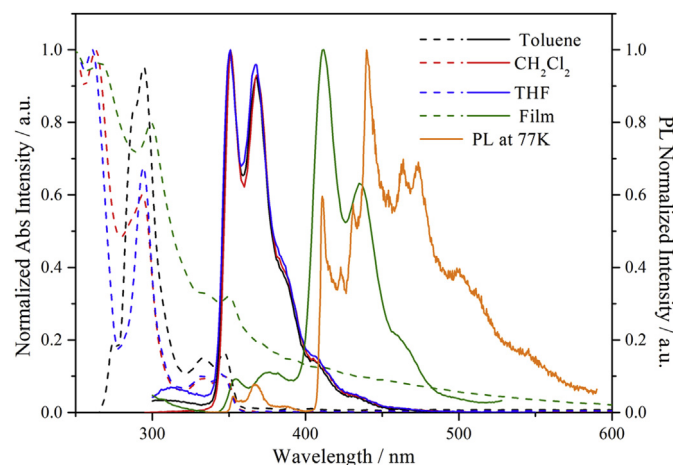


Fig. 1. UV-vis absorption and emission spectra in toluene, CH_2Cl_2 , THF solutions (10^{-5} M), neat thin film at room temperature and phosphorescence spectra in 2-MeTHF solutions (10^{-5} M) at 77 K with 1 ms delay.

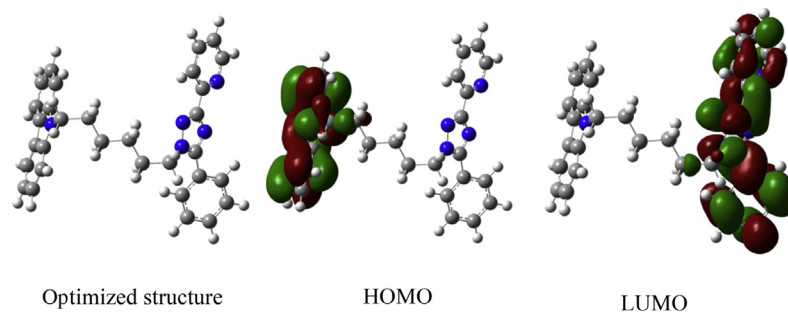


Fig. 2. The optimized molecular structure and frontier molecular orbitals (HOMO and LUMO) distribution for PPHCz.

Table 1
Photophysical properties of PPHCz

Compound	Abs peaks (nm)		Emission (nm)			T_d (°C)	HOMO (eV)	E_g (eV) ^d
	Solution ^a	Film ^b	Solution	Film	77 K ^c			
PPHCz	290, 336, 347	299, 333, 349	350, 367	353, 374, 411, 435,	411, 435, 439, 463, 473	330	–6.0	3.57

^a Measured in CH₂Cl₂ solution (1×10^{-5} M).

^b Films were made on quartz substrates with thicknesses of 80 nm.

^c Measured in 2-MeTHF at 77 K.

^d Determined from UV-visible absorption and emission spectra in CH₂Cl₂.

EL Elemental analyzer. UV–vis absorption spectra were recorded by Lambda Bio 40. The Photoluminescence (PL) spectra in different solutions and in thin film were examined by HORIBA FluouoMax-4 spectrophotometer. The low-temperature phosphorescence spectra were measured on an Edinburgh F-980 spectrometer at 77 K in 2-methyltetrahydrofuran (2-MeTHF). The thin solid films used for absorption and PL spectra measurements were vacuum vapor deposited on quartz substrates with thickness of 80 nm. Thermogravimetric analysis (TGA) was undertaken using a Netzsch TG 209F3 under dry nitrogen atmosphere heating at a rate of 10 °C/min.

Theoretical calculation of PPHCz was carried out by using the Gaussian 03 package. The ground state structure were optimized by density functional theory (DFT) in B3LYP/6-31G(d) basis sets. Theoretical prediction for molecular orbital distributions of PPHCz was acquired based on the optimized structure.

Cyclic voltammetry (CV) was carried out in CH₂Cl₂ solution with chromatographic purity at room temperature using a CHI 660E voltammetry analyzer. Tetrabutylammonium hexafluorophosphate (TBAPF6) (0.1 M) was used as the supporting electrolyte. The platinum wire is used as working electrode. The platinum electrode

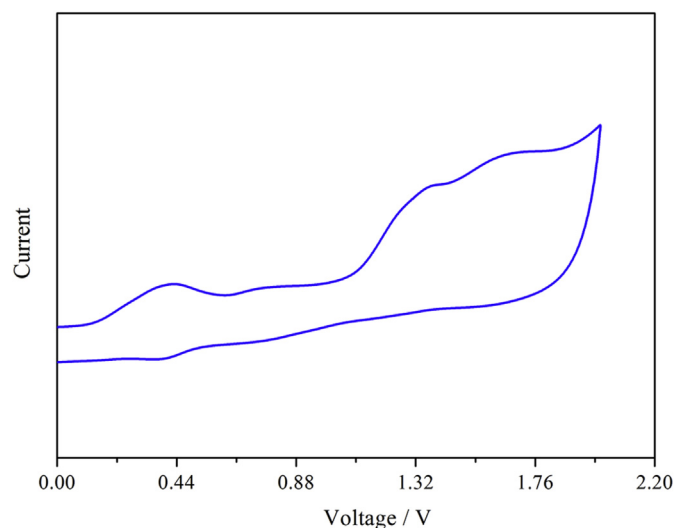


Fig. 4. Cyclic voltammograms in CH₂Cl₂ for oxidation.

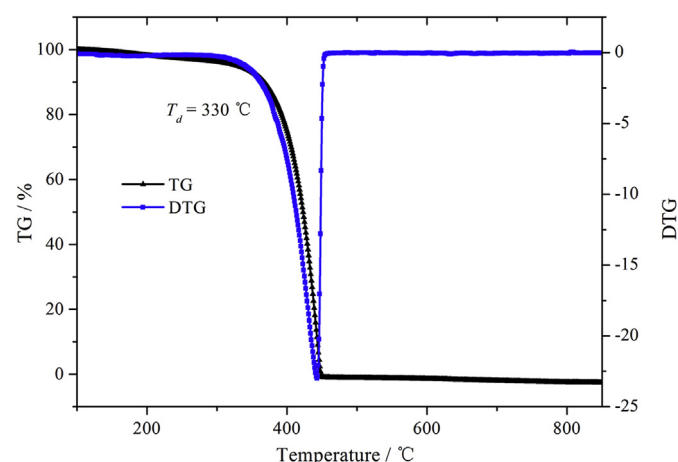


Fig. 3. TGA and DTG curves of HPPCz.

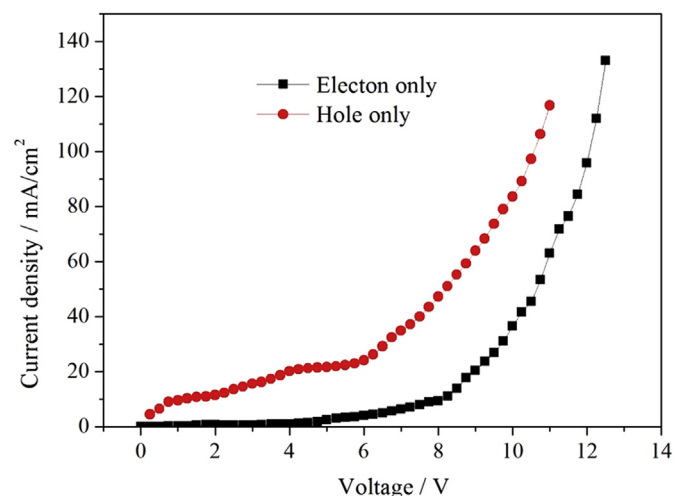


Fig. 5. Current density-voltage curves of hole- and electron-only devices of PPHCz.

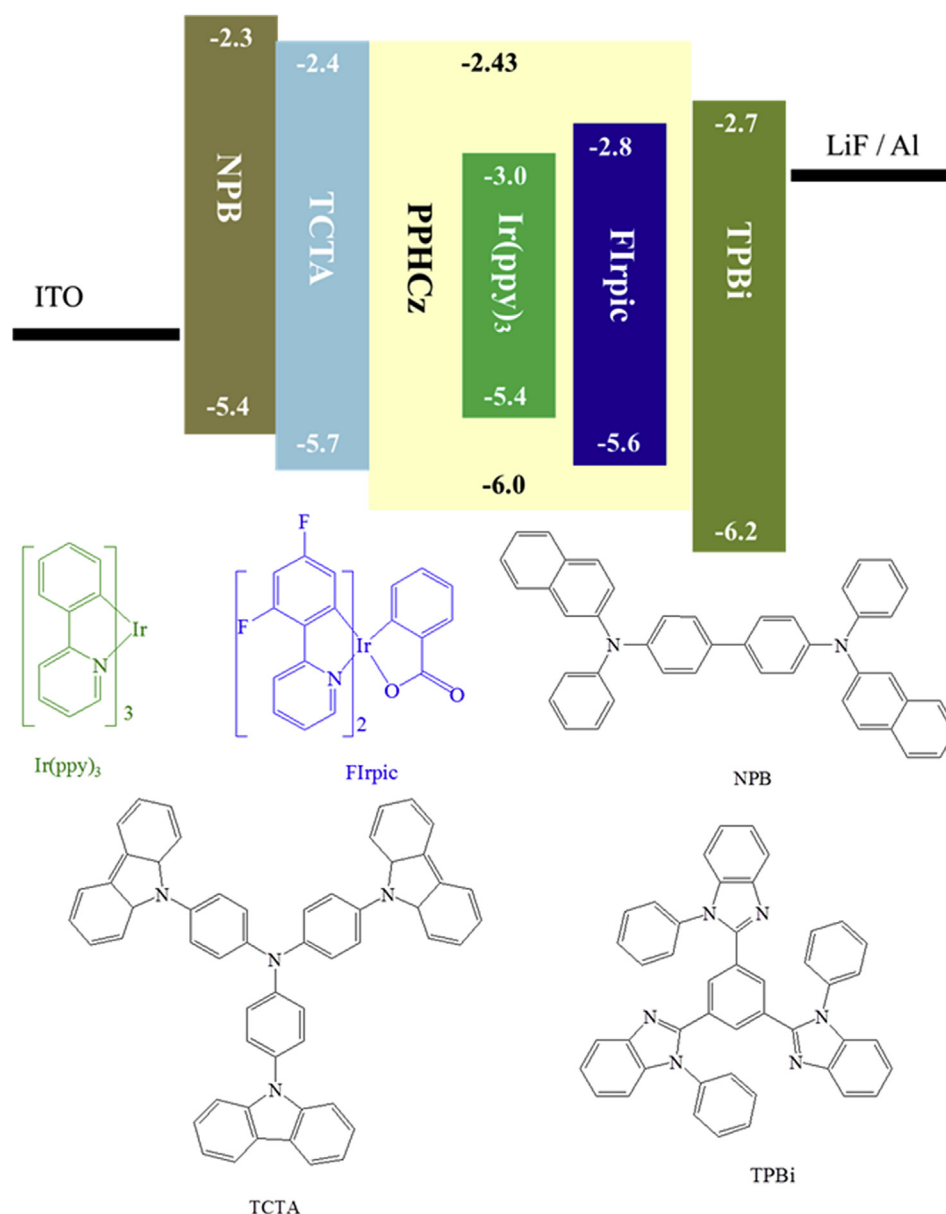


Fig. 6. Energy levels diagram of PhOLEDs and molecular structures of materials.

is the counter and a calomel electrode is the reference with ferrocenium-ferrocene (Fc^+/Fc) as the internal standard. The scan rate for CV curves is 100 mV/s.

Devices with area of $3 \times 3 \text{ mm}^2$ were fabricated by vacuum deposition ($3 \times 10^{-4} \text{ Pa}$) onto indium tin oxide (ITO) glass substrate. The ITO glass substrate was cleaned with deionized water, acetone, and ethanol in turn, and dried. To evaluate the bipolar property of PPHCz, the hole- and electron-only devices were fabricated with the structures ITO/NPB(20 nm)/PPHCz(30 nm)/NPB(20 nm)/Al(200 nm) and ITO/TPBi(20 nm)/PPHCz(30 nm)/TPBi(20 nm)/LiF(1 nm)/Al(200 nm). And then the green- and blue-emitting devices were fabricated by using *fac*-tris(2-phenylpyridine)iridium $\text{Ir}(\text{ppy})_3$ and iridium(III)bis(4,6-(difluorophenyl)pyridinato-N,C^{2'})picolinate (FIrpic) as dopants. The electroluminescent (EL) spectra and CIE coordinates were measured by PR-655 spectrophotometer. The voltage–current density (V–J) characteristics of PhOLEDs were recorded using Keithley 2400 Source Meter and ST-900M Spot Brightness Meter.

3. Characterization of materials

3.1. Photophysical properties

UV–vis absorption spectra of PPHCz in dilute toluene, CH_2Cl_2 and tetrahydrofuran (THF) solutions show the similar absorptions where the bands around 293, 331 and 345 nm, are displayed in Fig. 1. The absorption around 293 nm can be attributed to the $\pi-\pi^*$ transition local electron transition of carbazole and triazole. The absorption peaks at 331 and 345 nm can be assigned to the $n-\pi^*$ transitions of carbazoles.¹² The E_g calculated from the interaction absorption and PL spectra in CH_2Cl_2 solution of PPHCz is 3.57 eV.

Both absorption and fluorescence spectra of PPHCz are studied in different solutions with different polarities to detect solvatochromic possibility. Upon optical excitation at 290 nm, the maximum peaks at emission spectra of PPHCz in solutions are located at 351 and 367 nm with the much weaker peaks at 411 and 435 nm. The absorption and emission spectra in different solutions

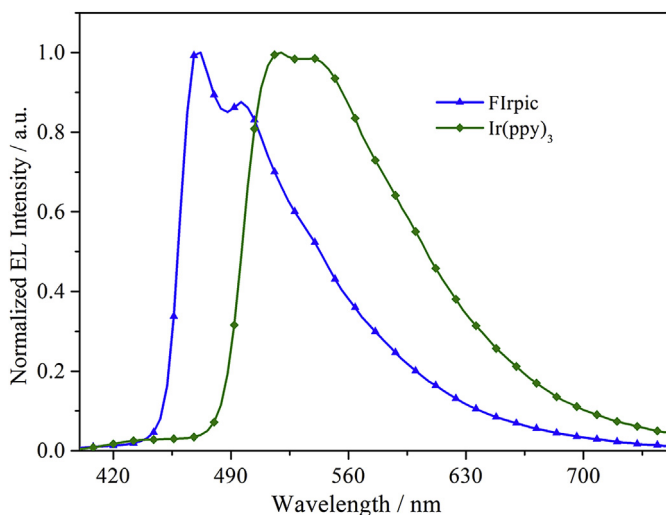


Fig. 7. EL spectra of green and blue devices at voltage of 8 V.

almost do not change with solvent polarity, indicating that no significant charge-transfer from donor to acceptor occurs due to the introduction of non-conjugate hexyl. In order to verify this point, the molecular structure of PPHCz was optimized by means of the B3LYP with the 6-31G (d) basis set and the electronic distributions of HOMO and LUMO are displayed in Fig. 2 (HOMO: the highest occupied molecular orbital; LUMO: the lowest unoccupied molecular orbital). HOMO is mainly distributed on the carbazole. While, LUMO dominates all on the 2-(5-phenyl-4H-1,2,4-triazol-3-yl)pyridine. There is little distribution on the hexyl, indicated that hexyl can break the conjugation between electron-donating and electron-withdrawing moieties in this compound.

However, a pronounced change is detected in fluorescence spectra of thin film. The emission peaks of thin film at 411 and 435 nm become stronger than that at 351 and 367, suggesting that the intermolecular interactions occur in solid state. To obtain triplet emission, the low-temperature PL spectrum was measured in a frozen 2-methyltetrahydrofuran matrix at 77 K and is also shown in Fig. 1. The emission bands below 411 nm should be assigned the fluorescence from the singlet excited state compared with the PL in thin film at room temperature. The fluorescence spectrum at 77 K exhibits the well-defined vibronic peaks, which is reported in other host materials.¹⁷ Therefore, E_T was estimated from the highest-

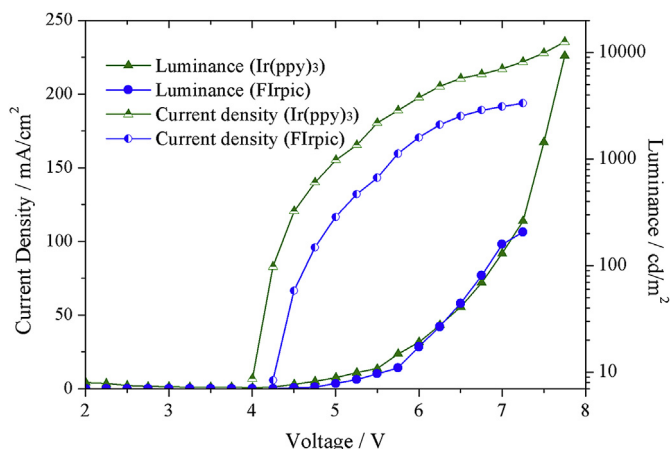


Fig. 8. Voltage-current density-luminance characteristics for PhOLEDs.

energy of the phosphorescence spectrum as 3.01 eV. All spectra data are summary in Table 1.

3.2. Thermal property

The thermal stability of PPHCz was examined by TGA and DTG. As displayed in Fig. 3, its onset decomposition temperature (T_d , corresponding to 5% weight loss) appears at 330 °C, indicating that PPHCz is favorable for fabrication of OLED devices by vacuum thermal evaporation.

3.3. Electrochemical property

The electrochemical property of PPHCz was studied in CH_2Cl_2 through CV, in Fig. 4. The HOMO energy level ($E_{\text{HOMO}} = -6.0$ eV) was calculated from equation of $E_{\text{HOMO}} = -4.8 - e(E_c^{\text{ox}} - E_f^{\text{ox}})\text{V}$, where E_c^{ox} was the first oxidation peaks measured from CV curves and was the oxidation peak of ferrocene ($E_c^{\text{ox}} = 1.6$ V and $E_f^{\text{ox}} = 0.4$ V). So, the LUMO energy level of $E_{\text{LUMO}} = -2.43$ eV was obtained by $E_{\text{LUMO}} = E_g - E_{\text{HOMO}}$.

3.4. Electroluminescent performances

To investigate the charge-transport property of PPHCz, we prepared electron- and hole-only devices with the structures of ITO/NPB(20 nm)/PPHCz(30 nm)/NPB(20 nm)/Al(200 nm) and ITO/TPBi(20 nm)/PPHCz(30 nm)/TPBi(20 nm)/LiF(1 nm)/Al(200 nm).

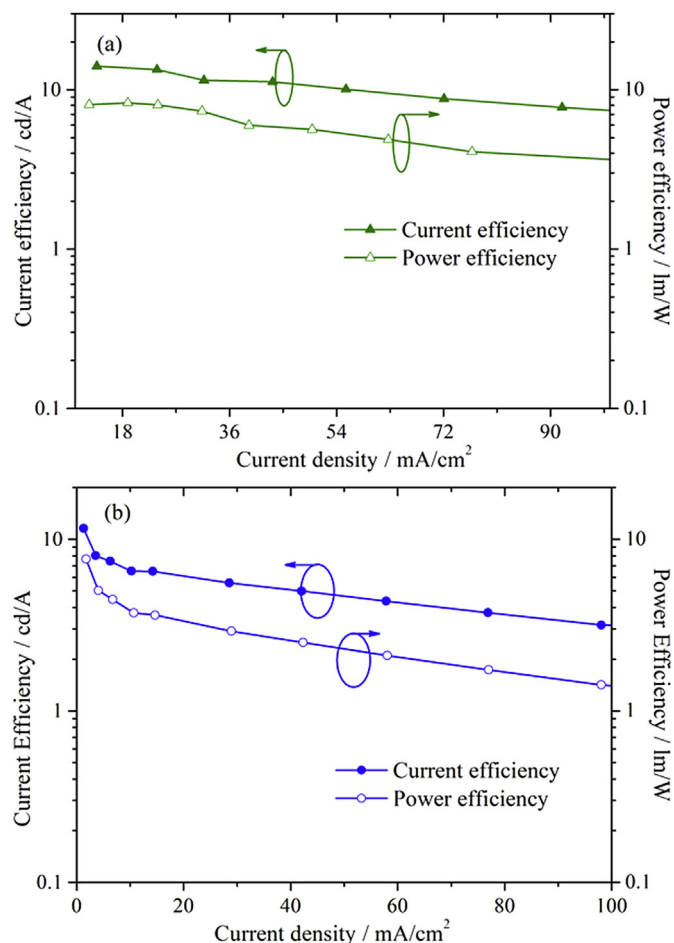


Fig. 9. Current efficiency-current density-power efficiency of green (a) and blue (b) PhOLEDs.

Table 2
EL performances of green and blue PhOLEDs

Dopant	λ_{max} (nm)	$V_{turn-on}$ (V)	L_{max} (cd/m ²)	$\eta_{c(max)}$ (cd/A)	η_p (max) (lm/W)	CIE (x, y)
Ir(ppy) ₃	515	4.0	12,597	14.0	8.0	0.37, 0.55
Flrpic	470, 496	4.2	3328	11.5	7.6	0.24, 0.40

NPB (N, N'-bis(naphthalen)-N,N'-bis(phenyl)-benzidine) was used as hole-transport layer; and TPBi [1,3,5-tris(2-Nphenylbenzimidazolyl)-benzene] were used as electron-transport materials. The hole and electron current density-voltage curves of PPHCz are shown in Fig. 5. The hole-only device exhibits higher carrier current density than the electron-only device at the same voltage due to the weak electron deficient group of 1,2,4-triazol and the strong electron donating of carbazole.

PPHCz was evaluated as the bipolar host material for green and blue PhOLEDs doped with Ir(ppy)₃ and Flrpic. The devices configurations were as follows: ITO/NPB (30 nm)/TCTA (10 nm)/PPHCz: Ir(ppy)₃ (6 %wt, 30 nm)/TPBi (35 nm)/LiF (1 nm)/Al (200 nm) and ITO/NPB (30 nm)/TCTA (10 nm)/PPHCz: Flrpic (8 %wt, 30 nm)/TPBi (35 nm)/LiF (1 nm)/Al (200 nm). NPB was used as hole-transport layer; and TPBi were used as electron-transport materials. TCTA [Tris(4-carbazoyl-9-ylphenyl)amine] can reduce the hole injection barrier from NPB to the host. The molecular structures of all materials and energy levels in PhOLEDs are displayed in Fig. 6.

The maximum peaks at EL spectra of green PhOLED is located at 515 nm with the CIE coordinate of (0.37, 0.55), which means a typical Ir(ppy)₃ emission feature. In blue device, the emission peaks of 470 and 496 nm were observed with CIE of (0.24, 0.40), which is consistent with PL of Flrpic,¹⁸ as shown in Fig. 7. There are no residual emission peaks from other functional layers suggests a complete energy transfer from host to dopant.

The current density–voltage–luminance (V–J–L) characteristics and efficiency versus current density curves of green- and blue-emitting PhOLEDs are shown in Figs. 8 and 9. The green device has a lower turn-on voltage ($V_{turn-on}$ =4.0 V, corresponding to 1 cd/m²) than that of blue-emitting device based Flrpic device (4.2 V). The green-emitting PhOLEDs exhibited a maximum luminance (L_{max}) of 12,597 cd/m² at 7.8 V, and a maximum current efficiency (η_c) of 14.0 cd/A, corresponding to a peak power efficiency (η_p) of 8.0 lm/W. The blue-emitting device based on Flrpic achieved L_{max} of 3328 cd/m², maximum η_c of 11.5 cd/A and maximum η_p of 7.6 lm/W, respectively. The detailed performances of green- and blue-emitting PhOLEDs are summarized in Table 2.

4. Conclusions

In summary, a novel bipolar green and blue host material of 9-(6-(3-phenyl-5-(pyridin-2-yl)-4H-1,2,4-triazol-4-yl)hexyl)-9H-carbazole (PPHCZ) has been designed and synthesized. The maximum

peaks at emission spectra of PPHCz in different solutions are located at 351, 367 nm and the emission peaks appeared at 353, 374, 411 and 435 nm in thin solid film. PPHCz exhibited the wide energy gap (3.57 eV). The blue PhOLED was fabricated using Flrpic as dopant and PPHCZ as host with the maximum luminance, maximum current and power efficiencies of 12,597 cd/m², 14.0 cd/A and 8.0 lm/W.

Acknowledgements

This work was financially supported by the International Science and Technology Cooperation Program of China (2012DFR50460); National Natural Science Foundation of China (21071108, 60976018, 61274056 and 61205179); Natural Science Foundation of Shanxi Province (2015021070); Program for Changjiang Scholar and Innovation Research Team in University (IRT0972); and Shanxi Provincial Key Innovative Research Team in Science and Technology (201513002-10).

References and notes

- Ho, C.-L.; Wong, W.-Y. *New J. Chem.* **2013**, *37*, 1665.
- Tao, P.; Li, W.-L.; Zhang, J.; Guo, S.; Zhao, Q.; Wang, H.; Wei, B.; Liu, S.-J.; Zhou, X. H.; Xu, B. S.; Huang, W. *Adv. Funt. Mater.* **2016**, *26*, 881.
- Yook, K. S.; Lee, J. Y. *Adv. Mater.* **2014**, *26*, 4218.
- Yin, X.; Zhang, T.; Peng, Q.; Zhou, T.; Zeng, W.; Zhu, Z.; Xie, G.; Li, F.; Ma, D.; Yang, C. *J. Mater. Chem. C* **2015**, *3*, 7589.
- Zhuang, J.; Li, W.; Su, W.; Liu, Y.; Shen, Q.; Liao, L.; Zhou, M. *Org. Electron.* **2012**, *13*, 2210.
- Kang, J. S.; Hong, T. R.; Kim, H. J.; Son, Y. H.; Bin, J. K.; Lee, B. S.; Yang, J. H.; Kim, J. W.; Cho, M. J.; Kwon, J. H.; Choi, D. H. *Org. Electron.* **2015**, *26*, 218.
- Chou, H. H.; Cheng, C.-H. *Adv. Mater.* **2010**, *22*, 2468.
- Han, C.; Zhang, Z. S.; Xu, H.; Xie, G. H.; Li, J.; Zhao, Y.; Deng, Z. P.; Liu, S. Y.; Yan, P. F. *Chem.—Eur. J.* **2013**, *19*, 141.
- Sapochak, L. S.; Padmaperuma, A. B.; Cai, X.; Male, J. L.; Burrows, P. E. *J. Phys. Chem. C* **2008**, *112*, 7989.
- Lee, Y.-T.; Chang, Y.-T.; Lee, M.-T.; Chiang, P.-H.; Chen, C.-T. *J. Mater. Chem. C* **2014**, *2*, 382.
- Xie, Y.-M.; Cui, L.-S.; Zu, F.-S.; Igbari, F.; Xue, M.-M.; Jiang, Z.-Q.; Liao, L.-S. *Org. Electron.* **2015**, *26*, 25.
- Mondal, E.; Hung, W.-Y.; Dai, H.-C.; Chen, H.-F.; Hung, P.-Y.; Wong, K. T. *Tetrahedron* **2014**, *70*, 6328.
- Kido, J.; Hongawa, K.; Okuyama, K.; Nagai, K. *Appl. Phys. Lett.* **1993**, *63*, 2627.
- Hung, M. C.; Liao, J. L.; Chen, S. A.; Chen, S. H.; Su, A. C. *J. Am. Chem. Soc.* **2005**, *127*, 14576.
- Zhuang, J.; Su, W.; Wu, W.; Li, W.; Shen, Q.; Zhou, M. *Tetrahedron* **2013**, *69*, 9038.
- Xu, H. X.; Yue, Y.; Qu, L. T.; Hao, Y. Y.; Wang, H.; Chen, L. Q. *Dyes Pigments* **2013**, *99*, 67.
- Li, W.; Li, J.; Liu, D.; Wang, F.; Zhang, S. *J. Mater. Chem. C* **2015**, *3*, 12529.
- Lee, J.; Park, H.; Park, K.-M.; Kim, J.; Lee, J.-Y.; Kang, Y. *Dyes Pigments* **2015**, *12*, 235.